ELSEVIER

Journal of Wind Engineering
and Industrial Aerodynamics 96 (2008) 1856–1870

JOURNAL OF wind engineering AND industrial aerodynamics

www.elsevier.com/locate/jweia

Identification of critical structural modes and flutter derivatives for predicting coupled bridge flutter

Xinzhong Chen[a,*], Ahsan Kareem[b]

[a]*Department of Civil and Environmental Engineering, Wind Science and Engineering Research Center, Texas Tech University, Lubbock, TX 79409, USA*

[b]*Department of Civil Engineering and Geological Sciences, NatHaz Modeling Laboratory, University of Notre Dame, Notre Dame, IN 46556, USA*

Available online 18 April 2008

Abstract

This study identifies the control parameters which critically influence the development of inter-modal coupling and the generation of aerodynamic damping, based on closed-form solutions of bimodal coupled analysis of bridge aerolastic system. This information helps in developing a guideline for the selection of most critical structural modes in a coupled flutter analysis and in better interpretation and understanding of the multimode coupled bridge flutter response. Also discussed is the role of each flutter derivative and the potential influence of the self-excited drag force on bridge flutter in light of the flutter features characterized by the rate of change in modal damping with increase in wind velocity, which is also referred to as soft- or hard-type flutter.

Keywords: Bridges; Flutter; Wind loads; Aerodynamics; Aeroelasticity; Dynamics

1. Introduction

In recent years, the necessity of considering aerodynamic coupling among multiple modes of bridge deck motion rather than only the fundamental vertical bending and torsional modes in the prediction of coupled bridge flutter has widely been recognized (e.g., Jones et al., 1998; Chen et al., 2000). The multimode coupled analysis framework offers a more accurate prediction of bridge flutter as compared to the traditional bimodal coupled

*Corresponding author.
E-mail address: xinzhong.chen@ttu.edu (X. Chen).

0167-6105/$ - see front matter
doi:10.1016/j.jweia.2008.02.025

framework. Many analysis examples have demonstrated that bridge flutter is dominated by a few important structural modes of deck vibration. From the point of view of flutter prediction with the multimode framework, the clarification of the most important modes for coupled flutter may not be an important issue, because the analysis even involving a larger number of modes, e.g., 50 modes, neither requires large computational resources nor is it cumbersome. However, improved understanding of the most important modes helps in better capturing the underlying physics of coupled flutter. It also offers equally valuable guidance for design and interpretation of wind tunnel studies using full aeroelastic bridge models which may only be able to replicate a limited number of selective modes of the prototype bridge due to difficulties in model fabrication and cost involved. These most important modes may be identified in a trial and error manner through the comparison of flutter analyses involving different mode combinations, or by their amplitudes in the flutter motion, or through their contributions to system damping (Chen et al., 2000). However, a simple and physically insightful guideline for the selection of bridge modes in a coupled flutter analysis has not been reported in the literature.

Another important issue in a flutter analysis concerns the modeling of self-excited forces. It has generally been understood that the self-excited lift and pitching moment acting on a bridge deck caused by vertical and torsional motions in terms of eight flutter derivatives, H_i^* and A_i^* ($i = 1-4$), play a most important role in the generation of coupled flutter. A variety of identification methods have been developed to experimentally quantify these flutter derivatives through either free or forced vibration test in a wind tunnel (e.g., Sarkar et al., 1994; Matsumoto et al., 1995; Chen and Kareem, 2004). However, experience of Akashi Kaikyo Bridge has revealed that the drag force induced by the torsional displacement resulted in a considerable level of negative damping at higher wind velocities, which markedly contributed to the generation of coupled flutter (Miyata et al., 1994). This interesting finding has raised awareness to the modeling and quantification of the self-excited drag force and its potential importance to bridge flutter (e.g., Jones et al., 1998, 2002; Katsuchi et al., 1998; Chen et al., 2002). As a result, the traditional modeling of self-excited forces involving eight flutter derivatives have been extended to include total 18 flutter derivatives, i.e., H_i^*, P_i^* and A_i^* ($i = 1-6$). While this increasingly prevalent modeling is expected to result in better flutter prediction, it considerably complicates and undermines the efforts of better capturing the fundamental flutter characteristics of bridge deck sections with a minimum number of flutter derivatives (Matsumoto, 1999; Chen and Kareem, 2006; Chen, 2007). The importance of these additional flutter derivatives has been reported in a very limited number of bridge examples. However, many examples, on the other hand, have demonstrated that traditional modeling with eight flutter derivatives serves an adequate description of the self-excited forces and leads to an accurate prediction of flutter. Clearly, whether or not these additional flutter derivatives play an important role in the flutter prediction depends on the bridge structural dynamics and its aerodynamic characteristics. Accordingly, it becomes an important issue to clarify why and under what conditions these additional flutter derivatives can be excluded in a flutter analysis. Furthermore, even in case involving the traditional modeling with eight flutter derivatives, it has been well recognized that all these flutter derivatives do not play an equally important role in flutter prediction.

In this paper, the aerodynamic coupling of two modes are discussed using closed-form formulations, which reveals control parameters that most influence the inter-modal coupling and aerodynamic damping. This discussion leads to improved understanding of

the most important modes in a multimode coupled flutter. Based on the closed-form solution of bimodal coupled flutter, the role of each flutter derivative on coupled bridge flutter is identified, which clarifies why and under what conditions the modeling of self-excited forces can be simplified with a small number of most important flutter derivatives.

2. Equations of bridge motion

The bridge deck dynamic displacements in the vertical, lateral and torsional directions, i.e., $h(x,t)$, $p(x,t)$ and $\alpha(x,t)$, respectively, about its statically displaced position, are expressed as

$$h(x,t)=\sum_j h_j(x)q_j(t),\quad p(x,t)=\sum_j p_j(x)q_j(t),\quad \alpha(x,t)=\sum_j \alpha_j(x)q_j(t), \tag{1}$$

where $h_j(x)$, $p_j(x)$ and $\alpha_j(x)$ are the jth mode shapes in each respective direction; $q_j(t)$ is the jth modal coordinate; and x is the spanwise position.

The self-excited forces per unit length linearized around the statically displaced position, i.e., lift (downward), drag (downwind) and pitching moment (nose-up), are given in terms of the 18 flutter derivatives as (e.g., Scanlan, 1993)

$$L_{se}(t)=\frac{1}{2}\rho U^2(2b)\left(kH_1^*\frac{\dot h}{U}+kH_2^*\frac{b\dot\alpha}{U}+k^2H_3^*\alpha+k^2H_4^*\frac{h}{b}+kH_5^*\frac{\dot p}{U}+k^2H_6^*\frac{p}{b}\right), \tag{2}$$

$$D_{se}(t)=\frac{1}{2}\rho U^2(2b)\left(kP_1^*\frac{\dot p}{U}+kP_2^*\frac{b\dot\alpha}{U}+k^2P_3^*\alpha+k^2P_4^*\frac{p}{b}+kP_5^*\frac{\dot h}{U}+k^2P_6^*\frac{h}{b}\right), \tag{3}$$

$$M_{se}(t)=\frac{1}{2}\rho U^2(2b^2)\left(kA_1^*\frac{\dot h}{U}+kA_2^*\frac{b\dot\alpha}{U}+k^2A_3^*\alpha+k^2A_4^*\frac{h}{b}+kA_5^*\frac{\dot p}{U}+k^2A_6^*\frac{p}{b}\right), \tag{4}$$

where ρ is the air density; U is the mean wind velocity; $B=2b$ is the bridge deck width; $k=\omega b/U$ is the reduced frequency; ω is the frequency of motion; and H_j^*, P_j^* and A_j^* ($j=1-6$) are the flutter derivatives that are functions of reduced frequency.

The governing matrix equation of bridge motions in terms of modal coordinates excluding the buffeting forces is given by

$$\mathbf{M}\ddot{\mathbf{q}}+\mathbf{C}\dot{\mathbf{q}}+\mathbf{K}\mathbf{q}=\frac{1}{2}\rho U^2\left(\mathbf{A}_s\mathbf{q}+\frac{b}{U}\mathbf{A}_d\dot{\mathbf{q}}\right), \tag{5}$$

where $\mathbf{M}=\mathrm{diag}[m_j]$, $\mathbf{C}=\mathrm{diag}[2m_j\xi_{sj}\omega_{sj}]$ and $\mathbf{K}=\mathrm{diag}[m_j\omega_{sj}^2]$ are the generalized mass, damping and stiffness matrices, respectively; m_j,ξ_{sj} and ω_{sj} are the jth modal mass, damping ratio and frequency; $\mathbf{A}_s$ and $\mathbf{A}_d$ are the aerodynamic stiffness and damping matrices, respectively, and their elements pertaining to the i and jth modes are given by

$$\begin{aligned}A_{sij}=(2k^2)(&H_4^*G_{h_ih_j}+H_6^*G_{h_ip_j}+bH_3^*G_{h_i\alpha_j}+P_6^*G_{p_ih_j}+P_4^*G_{p_ip_j}+bP_3^*G_{p_i\alpha_j}\\&+bA_4^*G_{\alpha_ih_j}+bA_6^*G_{\alpha_ip_j}+b^2A_3^*G_{\alpha_i\alpha_j}),\end{aligned} \tag{6}$$

$$\begin{aligned}A_{dij}=(2k)(&H_1^*G_{h_ih_j}+H_5^*G_{h_ip_j}+bH_2^*G_{h_i\alpha_j}+P_5^*G_{p_ih_j}+P_1^*G_{p_ip_j}+bP_2^*G_{p_i\alpha_j}\\&+bA_1^*G_{\alpha_ih_j}+bA_5^*G_{\alpha_ip_j}+b^2A_2^*G_{\alpha_i\alpha_j})\end{aligned} \tag{7}$$

and

$$G_{r_i s_j} = \int_{\text{span}} r_i(x) s_j(x)\,\mathrm{d}x$$

(where $r, s = h, p, \alpha$) are the modal shape integrals.

The modal frequencies and damping ratios as well as inter-modal coupling of the bridge at a given wind velocity, with the contributions of aerodynamic stiffness and damping terms, can be analyzed through the solution of the following complex eigenvalue problem by setting $\mathbf{q}(t) = \mathbf{q}_0 \mathrm{e}^{\lambda t}$:

$$(\lambda^2 \mathbf{M} + \lambda \mathbf{C} + \mathbf{K})\mathbf{q}_0 \mathrm{e}^{\lambda t} = \tfrac{1}{2}\rho U^2 (\mathbf{A}_\mathrm{s} + \bar{\lambda}\mathbf{A}_\mathrm{d})\mathbf{q}_0 \mathrm{e}^{\lambda t}, \tag{8}$$

where $\lambda = -\xi\omega + \mathrm{i}\omega\sqrt{1-\xi^2}$; ξ and ω are the damping ratio and frequency of the complex modal branch of interest; $\bar{\lambda} = \lambda b/U = (-\xi + \mathrm{i}\sqrt{1-\xi^2})k$; and $\mathrm{i} = \sqrt{-1}$. The flutter condition is determined by seeking the critical flutter velocity that corresponds to zero damping.

3. Important structural modes for coupled bridge flutter

In order to reveal the control parameters which critically influence the development of inter-modal coupling and the generation of aerodynamic damping, the bimodal coupled bridge system is considered here. The aerodynamic stiffness and damping matrices are expressed as

$$\mathbf{A}_\mathrm{s} = (2k^2)\begin{bmatrix} B_{\mathrm{s}11} & B_{\mathrm{s}12} \\ B_{\mathrm{s}21} & B_{\mathrm{s}22} \end{bmatrix}, \quad \mathbf{A}_\mathrm{d} = (2k)\begin{bmatrix} B_{\mathrm{d}11} & B_{\mathrm{d}12} \\ B_{\mathrm{d}21} & B_{\mathrm{d}22} \end{bmatrix}, \tag{9}$$

where $B_{sij} = A_{sij}/(2k^2)$ and $B_{\mathrm{d}ij} = A_{\mathrm{d}ij}/(2k)$ $(i, j = 1, 2)$.

Assuming the system damping ratio ξ is low, the solutions of equation (8) can be given in terms of closed-form expressions (Chen and Kareem, 2006; Chen, 2007). The modal frequency and damping ratio and the coupled motion of these two modes in the modal branch with a higher frequency are determined as

$$\omega_2 = \omega_{\mathrm{s}2}(1 + \mu_2 B_{\mathrm{s}22} + \mu_1\mu_2\Phi_2' \cos\phi_2')^{-1/2}, \tag{10}$$

$$\xi_2 = \xi_{\mathrm{s}2}(\omega_{\mathrm{s}2}/\omega_2) - 0.5\mu_2 B_{\mathrm{d}22} - 0.5\mu_1\mu_2\Phi_2' \sin\phi_2', \tag{11}$$

$$q_{10}/q_{20} = \Phi_2 \mathrm{e}^{\mathrm{i}\phi_2} = \frac{\mu_1(B_{\mathrm{s}12} + \mathrm{i}B_{\mathrm{d}12})(\omega_2/\bar{\omega}_1)^2}{[1 - (\omega_2/\bar{\omega}_1)^2] + \mathrm{i}[2\bar{\xi}_1(\omega_2/\bar{\omega}_1)]}, \tag{12}$$

where

$$\Phi_2' = \sqrt{B_{\mathrm{s}12}^2 + B_{\mathrm{d}12}^2}\sqrt{B_{\mathrm{s}21}^2 + B_{\mathrm{d}21}^2}R_{\mathrm{d}2}, \tag{13}$$

$$\phi_2' = \tan^{-1}(B_{\mathrm{d}21}/B_{\mathrm{s}21}) + \phi_2, \tag{14}$$

$$\Phi_2 = \mu_1\sqrt{B_{\mathrm{s}12}^2 + B_{\mathrm{d}12}^2}R_{\mathrm{d}2}, \tag{15}$$

$$R_{\mathrm{d}2} = (\omega_2/\bar{\omega}_1)^2\{[1 - (\omega_2/\bar{\omega}_1)^2]^2 + [2\bar{\xi}_1(\omega_2/\bar{\omega}_1)]^2\}^{-1/2}, \tag{16}$$

$$\phi_2 = \tan^{-1}(B_{d12}/B_{s12}) - \tan^{-1}\{[2\bar{\xi}_1(\omega_2/\bar{\omega}_1)]/[1-(\omega_2/\bar{\omega}_1)^2]\}, \tag{17}$$

$$\bar{\omega}_1 = \omega_{s1}[1-\mu_1(\omega/\omega_{s1})^2 B_{s11}]^{1/2}, \tag{18}$$

$$\bar{\xi}_1 = \xi_{s1}(\omega_{s1}/\bar{\omega}_1) - 0.5\mu_1(\omega/\bar{\omega}_1)B_{d11} - \xi(\omega/\bar{\omega}_1) \tag{19}$$

and $\mu_1 = \rho b^2/m_1$ and $\mu_2 = \rho b^2/m_2$ are mass parameters and other quantities have been defined earlier.

Similarly, the closed-form solutions for the modal frequency and damping ratio of the other modal branch can be expressed as

$$\omega_1 = \omega_{s1}(1+\mu_1 B_{s11} + \mu_1\mu_2\Phi_1'\cos\phi_1')^{-1/2}, \tag{20}$$

$$\xi_1 = \xi_{s1}(\omega_{s1}/\omega_1) - 0.5\mu_1 B_{d11} - 0.5\mu_1\mu_2\Phi_1'\sin\phi_1', \tag{21}$$

where

$$\Phi_1' = \sqrt{B_{s12}^2 + B_{d12}^2}\sqrt{B_{s21}^2 + B_{d21}^2}R_{d1}, \tag{22}$$

$$\phi_1' = \tan^{-1}(B_{d12}/B_{s12}) + \phi_1, \tag{23}$$

$$R_{d1} = (\omega_1/\bar{\omega}_2)^2\{[1-(\omega_1/\bar{\omega}_2)^2]^2 + [2\bar{\xi}_2(\omega_1/\bar{\omega}_2)]^2\}^{-1/2}, \tag{24}$$

$$\phi_1 = \tan^{-1}(B_{d21}/B_{s21}) - \tan^{-1}\{[2\bar{\xi}_2(\omega_1/\bar{\omega}_2)]/[1-(\omega_1/\bar{\omega}_2)^2]\}, \tag{25}$$

$$\bar{\omega}_2 = \omega_{s2}[1-\mu_2(\omega/\omega_{s2})^2 B_{s22}]^{1/2}, \tag{26}$$

$$\bar{\xi}_2 = \xi_{s2}(\omega_{s2}/\bar{\omega}_2) - 0.5\mu_2(\omega/\bar{\omega}_2)B_{d22} - \xi(\omega/\bar{\omega}_2). \tag{27}$$

It is noted based on numerical studies that the influence of coupled aerodynamic terms on the modal frequencies of the coupled system are generally negligibly small. Therefore, the modal frequencies of the coupled system can be approximated by the frequencies of the corresponding uncoupled system as

$$\omega_1 \approx \bar{\omega}_1 \approx \omega_{10} = \omega_{s1}(1+\mu_1 B_{s11})^{-1/2}, \tag{28}$$

$$\omega_2 \approx \bar{\omega}_2 \approx \omega_{20} = \omega_{s2}(1+\mu_2 B_{s22})^{-1/2}. \tag{29}$$

From the preceding closed-form expressions, it is evident that the control parameters influencing the inter-modal coupling of two modes, especially, the modal damping, are the frequency ratio, damping ratios, mass parameters, coupled aerodynamic stiffness and damping terms between these two modes. Obviously, understanding these control parameters would help to develop a simple guideline for the selection of structural modes needed in a flutter analysis. As the coupled bridge flutter corresponds to a coupled motion of the fundamental torsional mode with other modes of the bridge deck motion, especially the vertical bending modes, the ensuing discussion focuses on the inter-modal coupling of the fundamental torsional mode with one vertical mode of the bridge deck motion. The mode shapes of the vertical bending and torsional modes are given as $h_1(x)\neq 0$, $p_1(x)=0$, $\alpha_1(x)=0$; $h_2(x)=0$, $p_2(x)\neq 0$, $\alpha_2(x)\neq 0$. When only the lift and pitching moment caused by the vertical and torsional motions are considered, the aerodynamic

matrices are expressed as

$$\mathbf{A}_s = (2k^2)\begin{bmatrix} H_4^* G_{h_1 h_1} & bH_3^* G_{h_1 \alpha_2} \\ bA_4^* G_{h_1 \alpha_2} & b^2 A_3^* G_{\alpha_2 \alpha_2} \end{bmatrix}, \quad \mathbf{A}_d = (2k)\begin{bmatrix} H_1^* G_{h_1 h_1} & bH_2^* G_{h_1 \alpha_2} \\ bA_1^* G_{h_1 \alpha_2} & b^2 A_2^* G_{\alpha_2 \alpha_2} \end{bmatrix}. \tag{30}$$

Clearly, a mode comprising large values of coupled aerodynamic stiffness and damping terms with the fundamental torsional mode is most likely to be important for coupled flutter. Furthermore, this coupling will be enhanced when its damping is low and its frequency is close to the torsional modal frequency. For example, the fundamental vertical bending mode often has higher similarity in mode shape with the fundamental torsional mode, which leads to larger coupled aerodynamic terms between these two modes. Therefore, the fundamental vertical bending mode is more likely to be coupled with the torsional mode than other higher vertical bending modes. The higher vertical bending modes have less similarity in their mode shapes with the fundamental torsional mode, although their frequencies may be closer to the torsional modal frequency. In this context, when the fundamental torsional mode is anti-symmetric, the corresponding fundamental bending mode is referred to as the fundamental anti-symmetric mode. Otherwise, both are referred to as fundamental symmetric modes. Some modes may become locally important in a certain wind velocity region where their frequencies are close to the frequency of flutter mode branch. Therefore, the modes that are most likely to be coupled with the fundamental torsional mode should be considered in the flutter analysis.

Figs. 1 and 2 show the predicted modal frequencies and damping ratios of a suspension bridge with a center span of nearly 2000 m. The flutter derivatives were determined using Theodorsen function. The structural damping ratio in each mode was assumed to be 0.0032. Analyses involving different combinations of structural modes were conducted where modes 2, 8 and 11 are the first, second and third symmetric vertical bending modes, mode 9 the second symmetric lateral bending mode, and mode 10 the first symmetric torsional mode. Fig. 3 shows the shapes of these modes in terms of the bridge deck deformations in three directions. For this suspension bridge, the fundamental vertical and torsional modes are symmetric rather than anti-symmetric. For the common three-span bridge with a symmetric layout, whether the fundamental mode will be symmetric or anti-symmetric depends on the general layout of the cable system, e.g., type, side-to-main span ratio, and supporting conditions (Gimsing, 1998). The bimodal flutter analysis that involves modes 2 and 8 results in a critical flutter velocity of 67.9 m/s, which is very close to

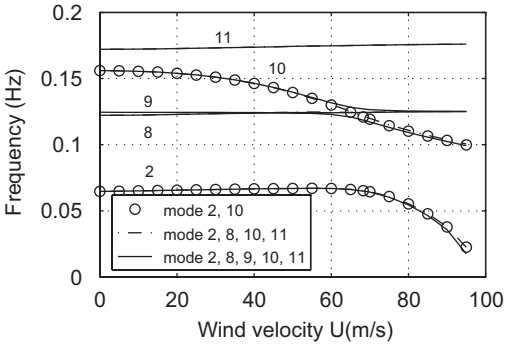

Fig. 1. Modal frequencies at varying wind velocities.

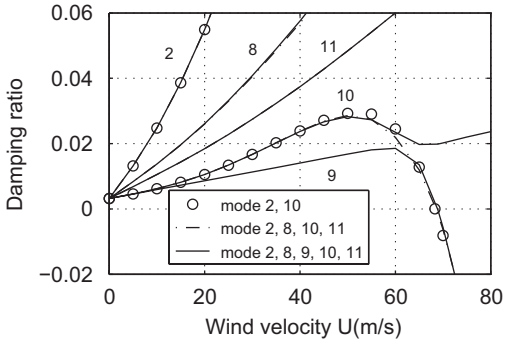

Fig. 2. Modal damping ratios at varying wind velocities.

69.3 m/s predicted when involving first 15 modes. Considering the curve veering of the frequency and damping loci of modal branches 9 and 10, the results involving multiple modes are consistent with that of the bimodal coupled system (Chen and Kareem, 2003a).

Fig. 4 shows the flutter motion in terms of the participation of structural modes with different amplitudes and phase angles. Fig. 5 shows the aerodynamic damping associated with the inter-modal coupling at the critical flutter velocity of 68.9 m/s when modes 2, 8, 9, 10 and 11 were considered in analysis. For instance, the term (2, 2) represents the damping when the bridge is vibrating in the single mode 2. The term (2, 10) indicates the damping attributed to the coupled terms of $\mathbf{A}_s$ and $\mathbf{A}_d$ relevant to modes 2 and 10. The summation of all these terms plus structural damping equal to zero at critical flutter velocity. Obviously, the two fundamental modes, modes 2 and 10, are most important modes in coupled flutter in light of their dominant contributions to system damping. The contributions of modes 9 and 10 to aerodynamic damping are relatively small and less important to flutter. Their large amplitudes are due to their resonance to coupled motion comprising modes 2 and 10 as their frequencies are close to the frequency of flutter motion. It is emphasized that the clarification of the modal contributions to the aerodynamic damping of the flutter mode branch instead of the flutter motion offers more accurate information regarding the role played by each structural mode in the generation of coupled flutter. It is also noted that the bimodal coupled flutter analysis that involves only the two fundamental modes remains a useful tool for quickly evaluating bridge flutter performance at preliminary design stage, specially for seeking best bridge deck sections with superior aerodynamic characteristics. The results of this bridge example concerning the important modes in coupled flutter can be readily interpreted by using the closed-form formulations.

4. Important flutter derivatives for coupled bridge flutter

For a bimodal coupled bridge system involving only the fundamental vertical and torsional modes, when only the self-excited lift and pitching moment are considered, the modal frequency and damping ratio of the torsional mode branch can be expressed as follows (Chen and Kareem, 2006; Chen, 2007):

$$\omega_2 = \omega_{s2}(1 + \upsilon A_3^* + \mu\upsilon D^2 \Psi' \cos\psi')^{-1/2}, \tag{31}$$

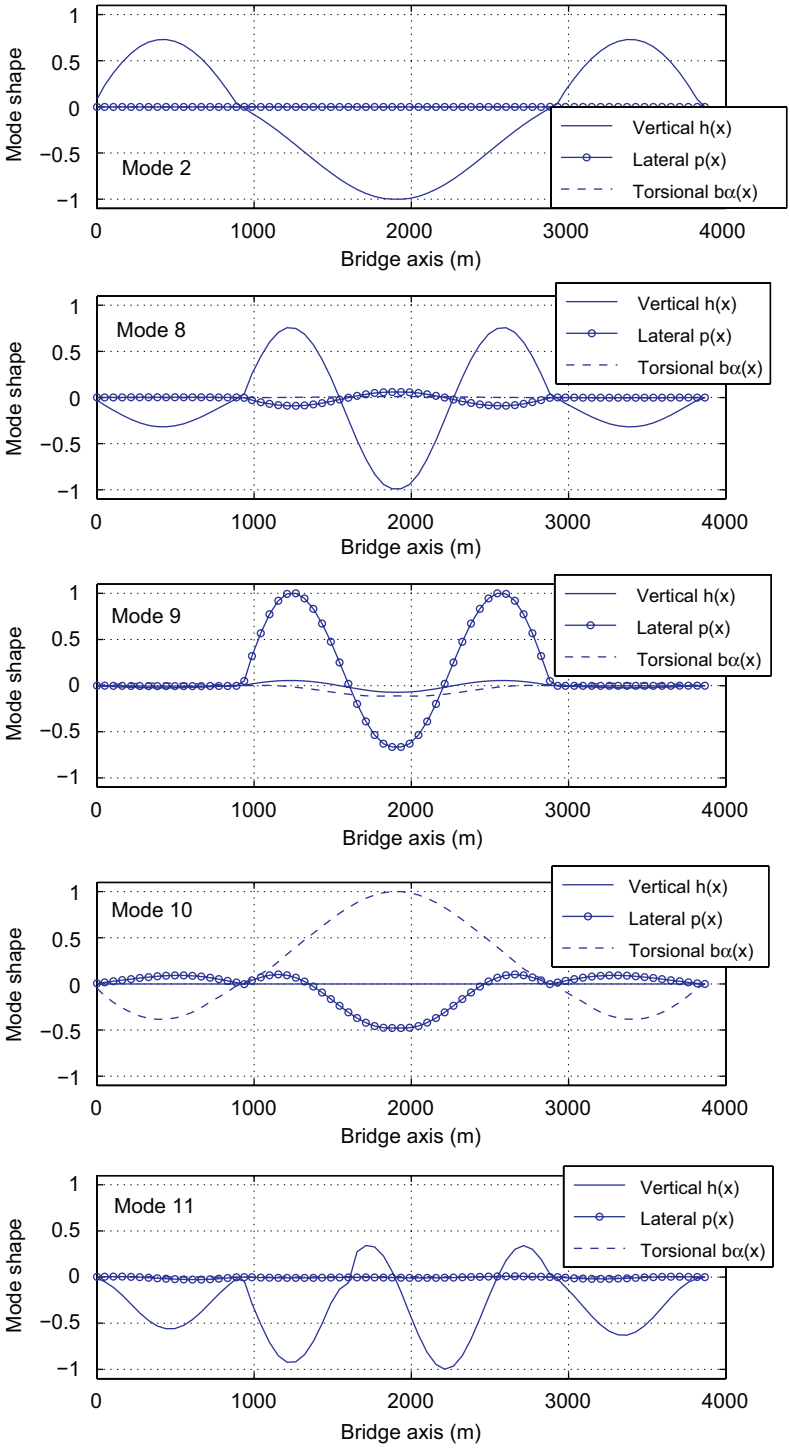

Fig. 3. Mode shapes of structural modes 2, 8, 9, 10 and 11 in terms of the bridge deck deformations in three directions.

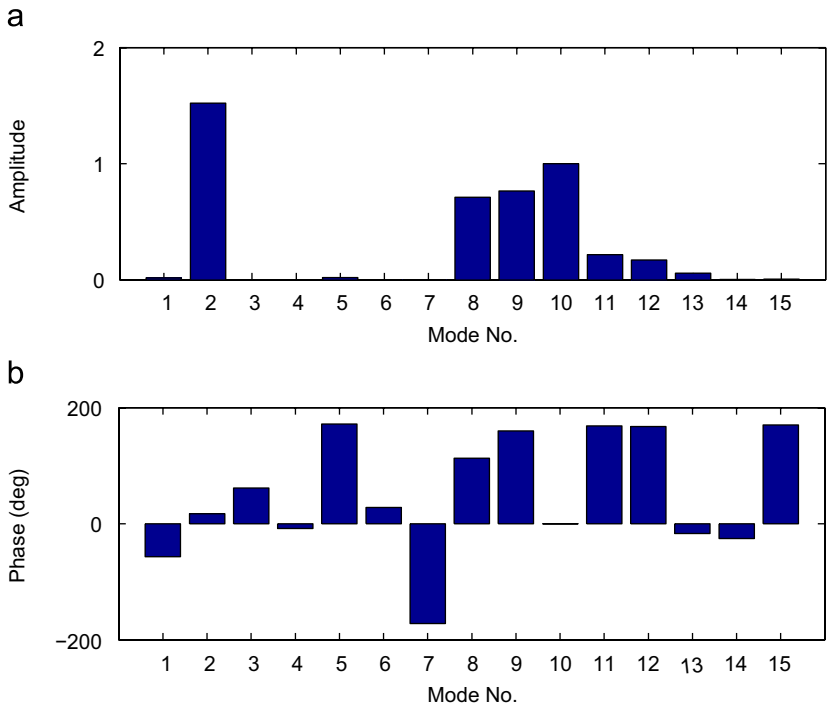

Fig. 4. Flutter motion in terms of the structural modal participation ($U = 69.3\,\mathrm{m/s}$): (a) amplitude ratios; (b) phase angles.

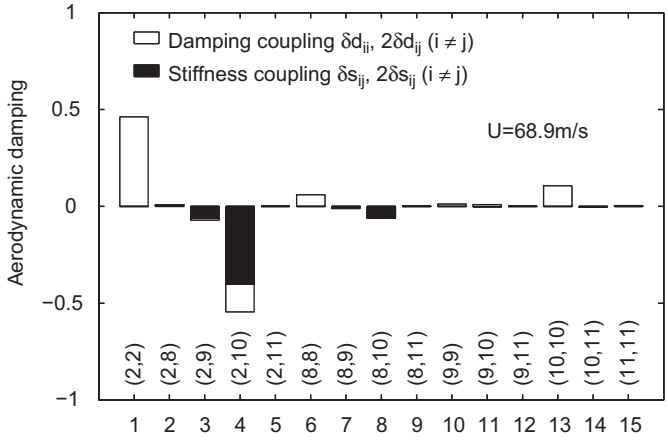

Fig. 5. Aerodynamic damping due to inter-modal aerodynamic coupling.

$$\xi_2 = \xi_{s2}(\omega_{s2}/\omega_2) - 0.5\upsilon A_2^* - 0.5\mu\upsilon D^2 \Psi' \sin\psi', \tag{32}$$

where

$$\Psi' = R_{d2}\{[(H_3^*)^2 + (H_2^*)^2][(A_4^*)^2 + (A_1^*)^2]\}^{1/2}, \tag{33}$$

$$\psi' = \tan^{-1}(A_1^*/A_4^*) + \tan^{-1}(H_2^*/H_3^*) - \tan^{-1}\{[2\bar{\xi}_1(\omega_2/\bar{\omega}_1)]/[1-(\omega_2/\bar{\omega}_1)^2]\}, \quad (34)$$

$\mu = \rho b^2/m$, $\upsilon = \rho b^4/I$, $m = m_1/G_{h_1h_1}$ and $I = m_2/G_{\alpha_2\alpha_2} = mr^2$ are the effective mass and polar moment of inertia per unit span, respectively; r is the radius of gyration of the cross-section; $D = G_{h_1\alpha_2}/(G_{h_1h_1}G_{\alpha_2\alpha_2})^{1/2}$ is the similarity factor between the vertical and torsional mode shapes.

In the case of well separated modal frequencies, the damping ratio of the torsional modal branch can be further simplified as

$$\xi_2 = \xi_{s2}(\omega_{s2}/\omega_{20}) - 0.5\upsilon A_2^* + 0.5\mu\upsilon D^2(H_3^*A_1^* + H_2^*A_4^*)/[1-(\omega_{10}/\omega_{20})^2], \quad (35)$$

where ω_{10} and ω_{20} are the modal frequencies of the corresponding uncoupled system:

$$\omega_{10} = \omega_{s1}(1+\mu H_4^*)^{-1/2}, \quad \omega_{20} = \omega_{s2}(1+\upsilon A_3^*)^{-1/2}. \quad (36)$$

These closed-form expressions explicitly unveil the role of different force components on the modal damping. Fig. 6 shows the role of aerodynamic forces on the damping ratios of vertical and torsional modal branches of the aforementioned suspension bridge. The uncoupled aerodynamic forces, i.e., the lift caused by vertical motion and the pitching moment caused by torsion in terms of H_1^*, H_4^*, A_2^* and A_3^*, result in positive damping to both the vertical and torsional modal branches. The effects of the coupled forces, i.e., the

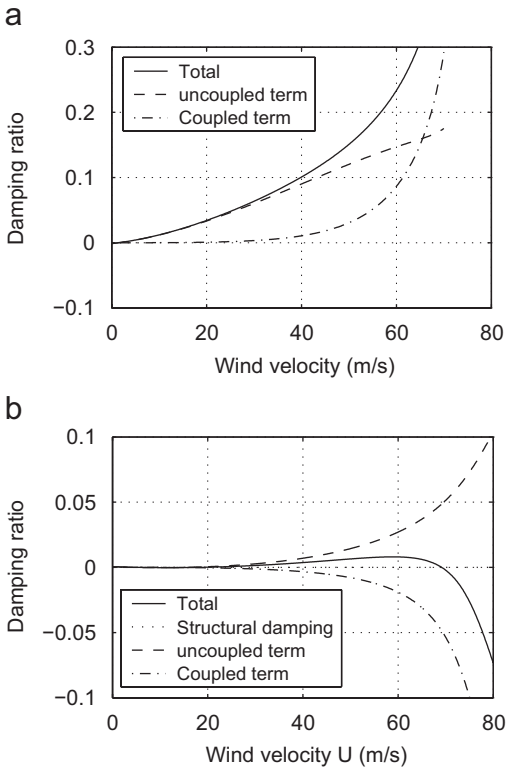

Fig. 6. Role of aerodynamic forces on modal damping (Box section): (a) vertical modal branch; (b) torsional modal branch.

lift caused by torsion and the pitching moment caused by vertical motion in terms of H_2^*, H_3^*, A_1^* and A_4^*, produce positive damping to the vertical modal branch but negative damping to the torsional modal branch. In the case in which the negative aerodynamic damping exceeds the positive aerodynamic and structural damping, the bridge becomes negatively damped which leads to the occurrence of flutter instability. For general slender bridge sections, $H_3^*A_1^* + H_2^*A_4^*$ is dominated by the value of $H_3^*A_1^*$, and the flutter derivatives H_3^*, A_1^*, A_2^* and A_3^* are most influential to coupled flutter.

Similar discussion on the role played by each flutter derivative can also be made when the self-excited forces are modeled in terms of 18 flutter derivatives. For the aforementioned bimodal coupled system involving the fundamental vertical and torsional modes, the aerodynamic stiffness and damping terms become

$$A_{s11} = (2k^2)H_4^*G_{h_1h_1}, \quad A_{d11} = (2k)H_1^*G_{h_1h_1},$$

$$A_{s12} = (2k^2)(H_6^*G_{h_1p_2} + bH_3^*G_{h_1\alpha_2}), \quad A_{d12} = (2k)(H_5^*G_{h_1p_2} + bH_2^*G_{h_1\alpha_2}),$$

$$A_{s21} = (2k^2)(P_6^*G_{h_1p_2} + bA_4^*G_{h_1\alpha_2}), \quad A_{d21} = (2k)(P_5^*G_{h_1p_2} + bA_1^*G_{h_1\alpha_2}),$$

$$A_{s22} = (2k^2)(P_4^*G_{p_2p_2} + bP_3^*G_{p_2\alpha_2} + bA_6^*G_{p_2\alpha_2} + b^2A_3^*G_{\alpha_2\alpha_2}),$$

$$A_{d22} = (2k)(P_1^*G_{p_2p_2} + bP_2^*G_{p_2\alpha_2} + bA_5^*G_{p_2\alpha_2} + b^2A_2^*G_{\alpha_2\alpha_2}). \tag{37}$$

Obviously, the importance of additional flutter derivatives on bridge flutter depends on their values and associated mode shape integrals. For instance, the contribution of P_1^*, P_2^* and A_5^* to A_{d22} can be regarded as an equivalent change in A_2^* given by $P_1^*G_{p_2p_2}/(b^2G_{\alpha_2\alpha_2}) + P_2^*G_{p_2\alpha_2}/(bG_{\alpha_2\alpha_2}) + A_5^*G_{p_2\alpha_2}/(bG_{\alpha_2\alpha_2})$. While this change is generally small in magnitude, it may have a markable effect on the critical flutter velocity when the value of A_2^* itself is low. Similar statements apply to other flutter derivatives.

To demonstrate the potential influence of drag force component on a coupled flutter, the following parametric study on the aforementioned suspension bridge is carried out. The modal integrals of the fundamental symmetric vertical and torsional modes are $G_{h_1h_1} = 1.1240\text{e}+03$, $G_{h_1p_2} = -0.3537\text{e}+03$, $bG_{h_1\alpha_2} = 1.1240\text{e}+03$, $G_{p_2p_2} = 0.1409\text{e}+03$, $bG_{p_2\alpha_2} = -0.3220\text{e}+03$ and $b^2G_{\alpha_2\alpha_2} = 0.9819\text{e}+03$. It is assumed that the lift and pitching moment caused by lateral motion are negligible, i.e., $H_5^* = H_6^* = A_5^* = A_6^* = 0$. The self-excited drag force is estimated by invoking the quasi-steady theory with the flutter derivatives given by (e.g., Chen and Kareem, 2002):

$$P_1^* = -2C_D/k, \quad P_2^* = 0.5(C'_D - C_L)/k, \quad P_3^* = C'_D/k^2, \quad P_5^* = (C'_D - C_L)/k \tag{38}$$

and $P_4^* = P_6^* = 0$ with $C_D = 0.3862$, $C'_D = 0.1200$ and $C_L = 0$. In this parametric study, three cases with different values of H_i^* and A_i^* ($i = 1-4$) are considered. Case A: H_i^* and A_i^* ($i = 1-4$) are determined through Theoderson function; Case B: H_i^* ($i = 1-4$) are the values of Case A divided by 5, and A_2^* and A_3^* are the values of Case A divided by 10; and Case C: H_i^* ($i = 1-4$), A_2^* and A_3^* are taken the values of Case A divided by 10.

Fig. 7 shows the equivalent changes in A_2^* and A_3^* as the results of considering P_i^* in the modeling of the self-excited forces. Fig. 8 portrays the influence of P_i^* on the modal frequencies and damping ratios at varying wind velocities. The effects of P_i^* ($i = 1-6$) on the critical flutter velocities are summarized in Table 1. The results of Cases B and C demonstrate that the influence of P_i^* on the critical flutter velocity may become noticeable

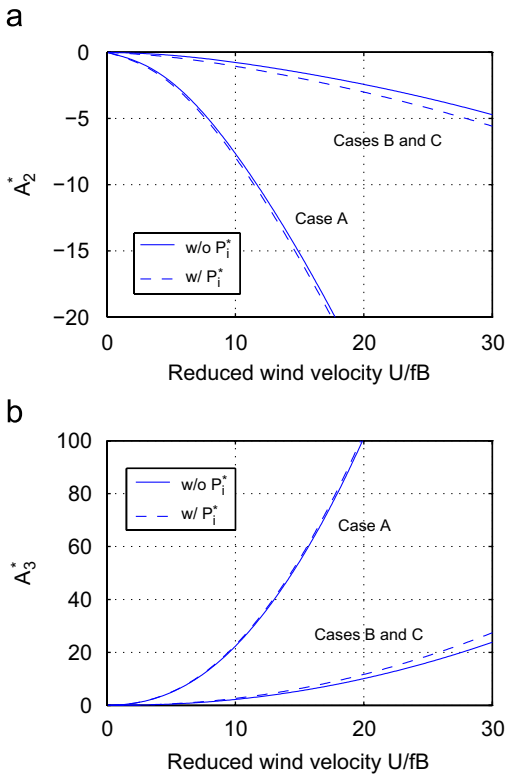

Fig. 7. Equivalent changes in flutter derivatives A_2^* and A_3^* due to P_i^*: (a) flutter derivative A_2^*; (b) flutter derivative A_3^*.

when their values are relatively large as compared to the traditional eight flutter derivatives. The effect of P_1^* is most significant which increases the modal damping and the critical flutter velocity. On the other hand, the results of Case A illustrate that for bridges with deck sections featured by large values of H_i^*, A_i^* $(i = 1-4)$, the effects of P_i^* are negligibly small.

The potential influence of the self-excited drag force on bridge flutter can be discussed in light of the flutter characteristics featured by the rate of change in the modal damping of the flutter modal branch with increasing wind velocity. In the case of a soft-type coupled flutter where the level of damping is low and it changes slowly with increasing wind velocity around the critical flutter velocity, even a little influence of additional self-excited drag force on the modal damping may result in a markable change in the predicted critical flutter velocity as indicated by Cases B and C. Consequently, careful modeling of the self-excited forces with the consideration of drag force may become critical for an accurate prediction of critical flutter velocity. The structural damping also becomes considerably beneficial to this type of flutter. However, majority of bridges are considered to exhibit a hard-type flutter characterized by modal damping that changes rapidly with increasing wind velocity around the flutter onset as indicated by Case A. This type of flutter typically associated with large values of self-excited lift and pitching moment caused by the vertical and torsional motion of bridge deck. For this type of flutter, the structural damping and

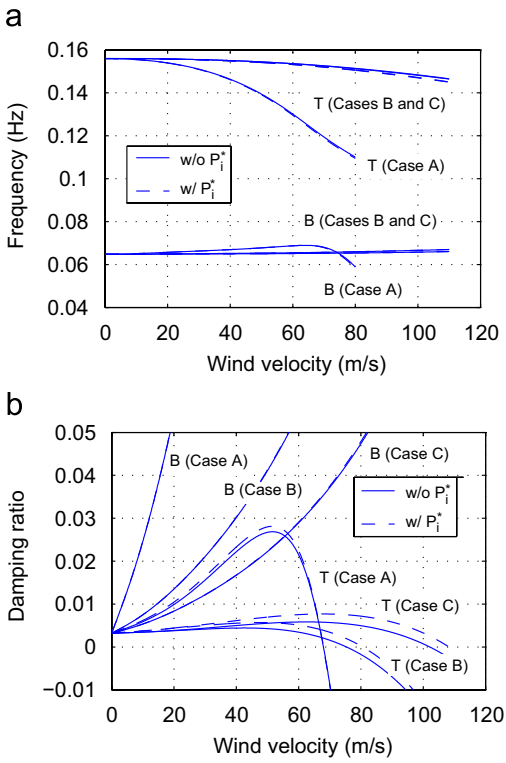

Fig. 8. Influence of P_i^* on the predicted modal frequencies and damping ratios: (a) modal frequencies; (b) modal damping ratios.

Table 1
Effect of P_i^* on critical flutter velocity

	w/o all P_i^*	w/all P_i^*	P_1^*	P_2^*, P_3^*, P_5^*	P_1^*, P_2^*	P_1^*, P_3^*	P_1^*, P_5^*
Structural modal damping ratios $\xi_{s1} = \xi_{s2} = 0$							
Case A	66.9	67.4	67.7	67.6	67.4	67.4	67.4
Case B	61.4	70.6	73.3	57.9	71.5	72.9	72.7
Case C	90.3	99.6	103.2	86.1	101.2	102.3	102.5
Structural modal damping ratios $\xi_{s1} = \xi_{s2} = 0.0032$							
Case A	67.9	67.9	68.6	67.3	68.5	68.3	68.3
Case B	75.4	80.6	82.8	73.1	81.5	82.3	82.2
Case C	102.1	108.2	111.6	98.8	110.0	111.4	111.8

the additional damping caused by the self-excited drag force or auxiliary damping through a tuned mass damper generally have a little effect on the critical flutter velocity (e.g., Chen and Kareem, 2003b).

To better understand the interesting result of Akashi Kaikyo Bridge concerning the effect of self-excited drag force on flutter, it is important to discuss the special feature of its truss deck section. This section is featured by a large value of static drag coefficient, C_D,

and small values of the derivatives of static lift and pitching moment coefficients with respect to angle of attack, C'_L and C'_M, as compared to a typical streamlined box section. In responding to the small values of C'_L and C'_M, the values of H_i^* and A_i^* ($i = 1-4$) are also small. Under the action of strong winds, this bridge shows a larger lateral deck deformation accompanied by a negative (nose-down) torsion. Around this statically deformed position with a negative angle of attack, the self-excited drag force particularly the component caused by torsional displacement in terms of P_3^* becomes noticeable, which is consistent with the large value of the derivative of drag coefficient with respect to angle of attack, C'_D. The effect of P_3^* results in an additional decrease in the modal frequency and the generation of negative aerodynamic damping which contribute to the occurrence of coupled flutter.

5. Concluding remarks

A simple guideline for selecting the most important structural modes in a coupled flutter analysis was presented in light of the control parameters which most influence the inter-modal coupling and more importantly the aerodynamic damping. The fundamental vertical bending and torsional modes are two dominant modes in a coupled flutter. The participation of other modes depends on their modal frequencies and the similarity in their mode shapes with the fundamental torsional mode.

The flutter derivatives H_3^*, A_1^*, A_2^* and A_3^* are the most important flutter derivatives that characterize the flutter performance of the section. The potential influence of the drag force on bridge flutter depends on the rate of change in modal damping with increasing wind velocity. For a soft-type flutter, additional aerodynamic damping of the drag force may have a markable influence on the critical flutter velocity. Consequently, careful modeling of the self-excited forces with the consideration of drag force may become critical for an accurate prediction of critical flutter velocity. However, a majority of bridges are characterized by a hard-type flutter, for which the effect of drag force is negligibly small. Therefore, inclusion of 18 flutter derivatives may not be necessarily important in these cases in light of the minimal improvement in the flutter prediction.

Acknowledgments

The authors would like to acknowledge the partial support provided by Robert M. Moran professorship and the start-up fund provided by Texas Tech University.

References

Chen, A., He, X., Xiang, H., 2002. Identification of 18 flutter derivatives of bridge decks. J. Wind Eng. Ind. Aerodyn. 90, 2007–2022.

Chen, X., 2007. Improved understanding of bimodal coupled bridge flutter based on closed-form solutions. J. Struct. Eng. 133 (1), 22–31.

Chen, X., Kareem, A., 2002. Advances in the modeling of aerodynamic forces on bridge decks. J. Eng. Mech. 128 (11), 1193–1205.

Chen, X., Kareem, A., 2003a. Curve veering of eigenvalue loci of bridges with aerodynamic effects. J. Eng. Mech. 129 (2), 146–159.

Chen, X., Kareem, A., 2003b. Efficacy of tuned mass damper for bridge flutter control. J. Struct. Eng. 129 (10), 1291–1300.

Chen, X., Kareem, A., 2004. Efficacy of the implied approximation in the identification of flutter derivatives. J. Eng. Mech. 130 (12), 2070–2074.

Chen, X., Kareem, A., 2006. Revisiting multimode coupled bridge flutter: some new insights. J. Eng. Mech. 132 (10), 1115–1123.

Chen, X., Matsumoto, M., Kareem, A., 2000. Aerodynamic coupling effects on flutter and buffeting of bridges. J. Eng. Mech. 126 (1), 17–26.

Gimsing, N.J., 1998. Cable Supported Bridges: Concept and Design, second ed. Wiley, New York.

Jones, N.P., Scanlan, R.H., Jain, A., Katsuchi, H., 1998. Advances (and challenges) in the prediction of long-span bridge response to wind. In: Larsen, A., Esdahl, S. (Eds.), Bridge Aerodynamics. Balkema, Rotterdam, The Netherlands, pp. 59–85.

Jones, N.P., Raggett, J.D., Ozkan, E., 2002. Prediction of cable-supported bridge response to wind: coupled flutter assessment during retrofit. J. Wind. Eng. Ind. Aerodyn. 91 (12–15), 1445–1464.

Katsuchi, H., Jones, N.P., Scanlan, R.H., 1998. Multimode coupled flutter and buffeting analysis of the Akashi-Kaikyo Bridge. J. Struct. Eng. 125 (1), 60–70.

Matsumoto, M., 1999. Recent study on bluff body aerodynamics and its mechanism. In: Larsen, Larose, Livesey (Eds.), Wind Engineering into the 21 Century. Balkema, Rotterdam, pp. 67–78.

Matsumoto, M., Niihara, Y., Kobayashi, Y., Shirato, H., Hamasaki, H., 1995. Flutter mechanism and its stabilization of bluff bodies. In: Proceedings of the Ninth ICWE, pp. 827–838.

Miyata, T., Tada, K., Sato, H., Katsuchi, H., Hikami, Y., 1994. New findings of coupled flutter in full model wind tunnel tests on the Akashi Kaikyo Bridge. In: Proceedings of the Symposium on Cable-Stayed and Suspension Bridges, Deauville, France, October 12–15, pp. 163-170.

Sarkar, P.P., Jones, N.P., Scanlan, R.H., 1994. Identification of aeroelastic parameters of flexible bridges. J. Eng. Mech. 120 (8), 1718–1742.

Scanlan, R.H., 1993. Problematics in formulation of wind-force models for bridge decks. J. Eng. Mech. 119 (7), 1353–1375.